Science of the Total Environment 835 (2022) 155485

Contents lists available at ScienceDirect

Science of the Total Environment

journal homepage: www.elsevier.com/locate/scitotenv

The use of surrogate standards as a QA/QC tool for routine analysis of microplastics in sewage sludge

Matthias Philipp [a], Thomas D. Bucheli [b], Ralf Kaegi [a,*]

[a] Eawag, Swiss Federal Institute of Aquatic Science and Technology, Überlandstrasse 133, CH-8600 Dübendorf, Switzerland
[b] Agroscope, Environmental Analytics, 8046, Zurich, Switzerland

HIGHLIGHTS

- Sewage sludge was spiked with different types of microplastic particles (MP).
- Colored polyethylene spheres were routinely used as surrogate standards.
- MP number and size were quantified with automated visible light microscopy & FT-IR.
- Sample specific extraction recoveries of MP were mostly >80%.

GRAPHICAL ABSTRACT

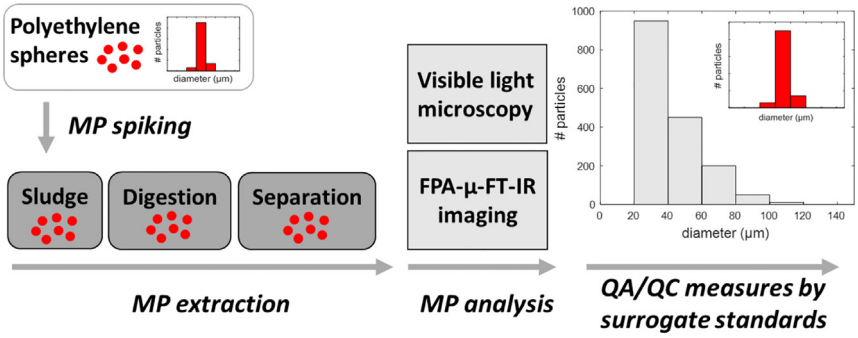

ARTICLE INFO

Editor: Damia Barcelo

Keywords:
Recovery
Sewage sludge
Microplastic
Sample preparation
Fourier-transform infrared spectroscopy
Optical microscopy

ABSTRACT

The efficient retention of microplastic particles (MP) during wastewater treatment results in their accumulation in the sewage sludge. Thus, sewage sludge represents a key matrix for understanding MP flows between engineered and natural systems. Building on previous reports, we present a sample preparation protocol optimized for digested sewage sludge. The key steps include acid digestion supported by Fenton reagents, enzymatic digestion, and density separation using sodium polytungstate (density of 1.9 gcm^{-3}). We use colored polyethylene (PE) spheres as surrogate standards to assess sample specific recoveries in terms of number and size, based on visible light (vis) microscopy and focal plane array - micro-Fourier transform - infrared (FPA-µ-FT-IR) imaging.

The FT-IR spectra of common MP were identical before and after the digestion procedures and morphological changes were observed for polylactide fibers only. Average recovery rates for PE spheres, polypropylene fibers and polyethylene terephthalate fragments extracted from spiked digested sewage sludge and determined using (automated) vis microscopy ranged from 80% to 100%. Similar recovery rates of around 80% were also obtained for PE spheres based on FPA-µ-FT-IR measurements. The median diameters of red and blue PE spheres in dry state and recovered from spiked deionized water and from extracts of spiked digested sewage sludge determined using vis microscopy ranged between 46 µm and 67 µm. These diameters were similar to 54 µm and 61 µm obtained from the FPA-µ-FT-IR measurements of the corresponding deionized water samples and digested sludge extracts and in line with data from the producer (53 µm–63 µm). Using our digestion protocol in combination with surrogate standards, we measured MP number concentrations of around 10,000 #/g in dried, digested sewage sludge, in agreement with recent results from other studies.

1. Introduction

Increasing production volumes, poor waste management practices and the persistence of synthetic polymers result in their unavoidable accumulation in the environment (Andrady, 2017; Barnes et al., 2009; Browne et al.,

* Corresponding author.
E-mail address: ralf.kaegi@eawag.ch (R. Kaegi).

http://dx.doi.org/10.1016/j.scitotenv.2022.155485
Received 31 January 2022; Received in revised form 6 April 2022; Accepted 20 April 2022
Available online 25 April 2022

2007; Geyer et al., 2017; Jambeck et al., 2015; Thompson et al., 2005). Consequently, synthetic polymers, here referred to as microplastic particles (MP) < 5 mm (Hartmann et al., 2019; Thompson et al., 2004) have been observed in natural ecosystems including the atmosphere (Beaurepaire et al., 2021), soils and sediments (Campanale et al., 2022; Duis and Coors, 2016; Horton et al., 2017; Kumar et al., 2020; Van Cauwenberghe et al., 2015; Zhou et al., 2020), aquatic environments (Andrady, 2011, 2017; Ivleva et al., 2017), as well as in technical systems such as wastewater treatment plants (WWTP) (Ben-David et al., 2021; Birch et al., 2020; Carr et al., 2016; Conley et al., 2019; Gatidou et al., 2019; Horton et al., 2021; Li et al., 2018; Mahon et al., 2017; Mintenig et al., 2017; Rasmussen et al., 2021; Talvitie et al., 2017), and in drinking water (Kirstein et al., 2021; Koelmans et al., 2019; Mintenig et al., 2019).

MP discharged to the wastewater are transported along the sewers systems and eventually reach a WWTP. In modern WWTP, the treatment starts with a bar screen of a few mm width, followed by the activated sludge process where MP attach to the biomass and are sedimented in secondary clarifiers. Additional sand filters installed to further increase the quality of the effluent water eliminate remaining MP from the wastewater. Several studies have investigated the retention of MP in full-scale WWTPs and reported removal efficiencies ranging from roughly 50%–100% with an average of around 85% (data compiled from Ali et al. (2021)). The considerable range of reported removal efficiencies is firstly related to different treatment schemes of the WWTPs (e.g., primary, secondary or tertiary treatment). Secondly, removal efficiencies are often derived by comparing MP concentrations in the influent and in the effluent of selected WWTPs as summarized by Ali et al. (2021), Gatidou et al. (2019) and Sun et al. (2019). Complex process schemes of WWTPs, however, make the assessment of the removal efficiencies based on influent and effluent MP concentrations a challenging task. In any case, the removal of MP from the wastewater stream results in the accumulation of MP in the sewage sludge. Anaerobic digestion conducted for energy production and volume reduction of the sludge (primary and secondary sludge) further enriches the MP content in the remaining solids. Thus, digested sewage sludge can be regarded as an efficient passive sampling system for MP, with considerably less temporal fluctuation of the MP content over time compared to the influent or effluent wastewater. For monitoring purposes assessing the MP content in digested sludge, thus, seems most rewarding. Different sample preparation protocols combined with different analytical methods having different size detection limits and degrees of automation, however, challenge the comparison of MP concentrations reported from different WWTP studies.

Various extraction protocols to isolate MP suitable for different matrices have been published, reviewed and are continuously modified (Blaesing and Amelung, 2018; Han et al., 2019; He et al., 2018; Horton et al., 2017; Junhao et al., 2021; Möller et al., 2021; Stock et al., 2019). Key elements of these sample preparation protocols are oxidative digestions using Fenton reagents, enzymatic digestions and density separation, combined in different ways and adjusted to different matrices. Preparation protocols suitable for sludge matrices have been presented and reviewed by various authors (Hurley et al., 2018; Leslie et al., 2017; Li et al., 2018; Mahon et al., 2017; Sujathan et al., 2017; Sun et al., 2019; Tagg et al., 2016). The transfer of analytes/MP from one sample processing media to another (e.g., from the oxidative digestion to the enzymatic digestion media) is generally achieved by filtration procedures using variable sizes of stainless steel sieves to isolate the particulate fraction of interest. These sample handling procedures may lead to a loss of MP.

For an unambiguous identification of the polymer type on an individual particle level, spectroscopic techniques, such as μ-FT-IR and μ-RAMAN are required (Anger et al., 2018; Birch et al., 2020; Hidalgo et al., 2006; Ivleva et al., 2017; Li et al., 2018; Moeller et al., 2020; Pico et al., 2019; Sun et al., 2019; Zhou et al., 2020). The focal plane array (FPA) technology in combination with a high degree of automation, makes the FPA-μ-FT-IR suitable for detecting, identifying and sizing individual MP particles deposited on suitable substrates (Löder et al., 2015; Mintenig et al., 2017; Primpke et al., 2017, 2018, 2020). For a quantitative assessment of the MP concentrations in complex (environmental) matrices, the sample specific MP recovery in terms of particle number and particle size is essential. However, despite the high degree of automation, sample specific MP recoveries were neither assessed nor reported in previous studies, making the interpretation of related experimental results challenging.

Based on results from previous studies (see citations above), we developed a sample preparation protocol optimized for digested sewage sludge. We used various MP types to test different process steps during the method development and to determine MP recoveries over the analytical chain. We subjected the most relevant MP polymer types to the developed extraction procedure and evaluated their chemical stabilities by attenuated total reflection (ATR)-μ-FT-IR measurements and determined morphological changes by visible light (vis) microscopy. Finally, we used colored PE spheres as surrogate standards to determine the sample specific MP recoveries in terms of number and size in routine application by automated vis microscopy and FPA-μ-FT-IR analysis.

2. Materials and methods

2.1. Chemicals

A list of all chemicals, including the brand, and their use in this study is provided in the supporting information (Table S1).

2.2. Microplastics

To assess changes in the MP's chemical (i.e. polymeric) structure and shape caused by the developed extraction protocol and to quantitatively determine the extraction efficiency of the method in terms of MP number and size, we selected MP of the polymer types and shapes specified in Table 1.

2.3. Sludge matrices

The focus of this work was on the extraction of MP from digested sewage sludge. Therefore, two sludges from different WWTP were selected (Werdhölzli (WH, Zuerich) with more than 400,000 connected inhabitants and Neugut (NG, Duebendorf), with about 40,000 connected inhabitants). Both WWTP have fine bar screens, primary and secondary clarification, and a biological wastewater treatment (activated sludge process) unit. The effluent from the secondary clarifier from both WWTP are treated with ozone and diverted through a sand filtration unit before being discharged into the surface water. The primary and the excess secondary sludge are anaerobically digested and dewatered, before being incinerated at the central mono incineration of WH. Digested sludge samples were collected from WH (30% total solids (TS)) and from NG (2% TS) for MP spiking experiments.

We expect that MP spiked as surrogate standards were characteristic enough to be distinguished from the MP already present in the digested sludge samples. Nevertheless, pristine (unspiked) sludge samples from WH and NG were prepared and analyzed the same way as the spiked samples to determine false positives of MP spiked as surrogate standards.

To assess false positives of any MP type and size, we used a (fresh) synthetic sewage sludge, consisting of a mixture of tap water (240 mL), feces (0.8 g), toilet paper (0.06 g) and urine (10 mL). This synthetic sludge underwent the same MP extraction protocol as the digested sludge that was collected from the WWTP. We are aware that our synthetic sludge may not be entirely plastic free as MP have been detected in human stool (Schwabl et al., 2019), however, at rather low concentrations of around 2 #/g. In the absence of a certified plastic free sewage sludge reference material, our synthetic sludge is, therefore, considered a viable option.

2.4. MP extraction protocol

Digested sewage sludge essentially consists of residual organic matter and contains high amounts of cellulose from toilet papers. High cellulose contents were also observed in raw wastewater samples (Simon et al.,

Table 1
List of microplastic particles (MP) that were used to assess (chemical) structural and morphological changes caused by the developed extraction protocol and to determine the sample specific MP recoveries. 'S' refers to MP used for the assessment of structural/morphological changes, 'RM' (recovery microscopy) refers to the sample specific recoveries determined using (automated) visible light microscopy, 'RIR' (recovery infrared) refers to the sample specific recoveries determined using FPA-μ-FT-IR imaging.

Polymer type	Form	Diameter (μm)	Length (mm)	Distributor	Use
Polyethylene terephthalate (PET)	Fragments (powder, white)	100–200	NA	PET-bottle (grinded, sieved)	S, RM
Polypropylene (PP)	Fibers (orange)	44	6	Baumhueter Extrusion GmbH, GER	S, RM
Polyethylene (PE)	Spheres (blue)	53–63	NA	Cospheric, CA, USA	S, RM, RIR
Polyethylene (PE)	Spheres (red)	53–63	NA	Cospheric, CA, USA	S, RM, RIR
Polymethylmethacrylate (PMMA)	Spheres (clear)	60	NA	NA	S
Polyvinylchloride (PVC)	Fragments (powder, white)	<300	NA	Goodfellow Cooperation, PA, USA	S
Polyethylene (PE)	Fibers (clear)	24	4.6	Baumhueter Extrusion GmbH, GER	S
Polylactide (PLA)	Fibers (clear)	13	4.6	Baumhueter Extrusion GmbH, GER	S

2018). As cellulose is neither degraded during the wastewater treatment (activated sludge process) nor during the sludge treatment (anaerobic digestion), it is accumulated in the digested sewage sludge. Wielinski et al. (2018) for example reported that roughly one third of the combustible materials in sewage sludge consisted of cellulose or hemicellulose. The ash content, representing inorganic materials including sand particles, varies between 30% and 50% (e.g., Fonts et al. (2009), Wielinski et al. (2018)). This makes the combination of an oxidative/enzymatic digestion and a density separation as parts of the sample preparation mandatory. Therefore, building on previous reports (Cole et al., 2014; Hurley et al., 2018; Mahon et al., 2017; Mintenig et al., 2017; Sujathan et al., 2017; Tagg et al., 2016), we developed an extraction protocol for MP that is tailored to digested sewage sludge matrices (Fig. 1) and allows for a quantitative evaluation of MP using vis microscopy and FPA-μ-FT-IR.

Glass beakers (250 mL) containing the spiked slurries of digested sewage sludge were covered with aluminum foil and freeze-dried. To avoid the evaporation of water and to limit the contamination, the beakers were also covered with aluminum foil during the following digestion steps. To mineralize the organic matter, an oxidative digestion step (Fig. 1) using Fenton reagents was carried out. For this purpose, 10 mL H_2O_2 (35%), 5 mL deionized (DI) water, 1 mL Fe(*II*)SO_4 (7 × H_2O, 2 mmol/L) and 1 mL protocatechuic acid (2 mmol/L) were added to 0.1 g or 1 g of freeze dried samples in a glass beaker. This mixture reacted on a horizontal shaker (Heidolph Incubator 1000/Unimax 1010) at 100 rpm in a fume hood at room temperature for 1 h. Afterwards, the temperature was set to 40 °C and the sample reacted for an additional 12 h. Due to high contents of organic material in the sludge, the oxidative digestion procedure was repeated by adding the same amounts of reagents to the digests and letting the suspension react for another 12 h at 40 °C. The resulting suspension was filtered through a 20 μm stainless steel sieve (diameter 47 mm, mesh 500, Zivipf.de). The beaker was rinsed 3 times with 50 mL DI water and the rinsing water was filtered through the same stainless steel sieve. The Fenton reagent efficiently mineralized easily degradable organic matter, but the cellulose fibers were still detected under the vis microscope. Therefore, the sludge extracts were additionally treated with cellulase enzymes (Fig. 1) as follows. The particle-loaded sieve was transferred to a glass beaker (250 mL) and incubated with 50 mL phosphate citrate buffer (50 mM, pH 5), 0.5 g cellulase (extracted from *Aspergillus niger*; Sigma-Aldrich, No. 22178) and 10 mg sodium azide at 40 °C on the same horizontal shaker (100 rpm). After a reaction time of 72 h, the stainless steel sieve was removed from the digests, rinsed from both sides using DI water, whereas the rinsing water was collected in the same beaker. The digest was filtered on the same, cleaned stainless steel sieve. The beaker was rinsed three times with 50 mL DI water and the rinse water was filtered over the same stainless steel sieve. However, despite the use of cellulase enzymes, cellulose was not fully mineralized and the remaining cellulose materials limited the amount of sludge extract eventually to be filtered on Al_2O_3 membranes for automated vis microscopy and FPA-μ-FT-IR imaging.

To separate the remaining inorganic particles from the MP, a density separation (Fig. 1) was performed using a sodium polytungstate (SPT, Roth, 8828) heavy liquid (15 mL). We used a density of 1.9 g/cm^3, which is above the density of commonly used plastics and allows including tire wear particles in future studies (Kloeckner et al., 2019). The stainless steel sieve containing the extracted particles was placed into a 120 mL glass beaker together with 15 mL SPT solution entirely covering the stainless steel sieve and the beaker was put into an ultrasonic bath (TP690-A, Bioblock Scientific) for 20 s. The SPT suspension was then transferred into a 50 mL centrifuge tube, the tube was closed and rotated for 1 h in an overhead shaker (30 rpm, Heidolph overhead shaker, type: Reax2). The well-mixed suspension was centrifuged at 2900 ×*g* for 45 min, and the supernatant was carefully decanted onto a sieve cascade (Fig. 1) (100 μm stainless steel sieve followed by a 20 μm stainless steel sieve), resulting in two size fractions. Particles >100 μm and fibers which were up to a few mm in length remained on the top stainless steel sieve. Fibers were, thus, excluded from the automated FPA-μ-FT-IR analysis. Even if we were able to remove the fibers from the stainless steel mesh and deposit them on an Al_2O_3 filter membrane, an automated analysis of the fibers would remain very challenging. Due to the complex 3 dimensional shape of the fibers only selected parts of the fibers would be in the focal plane of the IR laser and thus yield an interpretable spectrum. Particles between 20 μm and 100 μm were collected on the second sieve. This sieve was rinsed from both sides using DI water and the resulting suspensions were filtered on Al_2O_3 membranes (Anodisc, diameter 47 mm (extracts of 1 g sewage sludge), 25 mm (extracts of 0.1 g sewage sludge), pore size: 0.2 μm, Whatman®) for subsequent vis microscopy analysis and FPA-μ-FT-IR imaging. The rinsed sieves were inspected under the vis microscope to check for adhering particles.

2.5. Recovery assessment and quality assurance/quality control (QC/QA) measures

The MP-specific recovery rate was calculated as the ratio between spiked and recovered MP and is expressed in percent. Spiking experiments

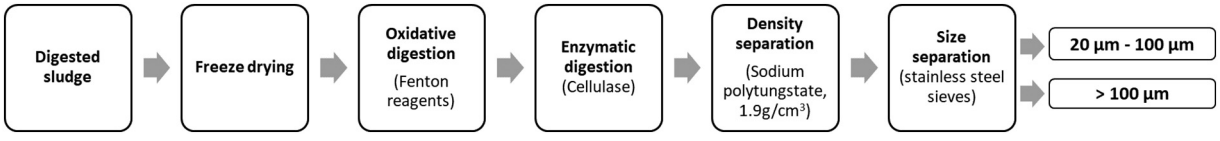

Fig. 1. Schematic of the different process steps applied to extract MP from sewage sludge matrices.

were conducted using DI water, digested sewage sludge and extracts thereof (Fig. 2).

2.5.1. DI water

The number and the size of the colored (red, blue) PE spheres deposited on glass slides in dry state were determined based on vis microscopy in combination with image analysis tools. The colored PE spheres transferred from the glass slides to DI water and filtered on Al_2O_3 membranes were investigated by both, vis microscopy and FPA-μ-FT-IR to determine their number and their size (Fig. 2).

2.5.2. Digested sewage sludge

To determine the MP recovery from digested sludge matrices, red PE spheres, PET fragments and PP fibers were jointly spiked to aliquots of the different sludge samples (Table S2) and blue PE spheres were spiked to digested sewage sludge after the enzymatic digestion but before the density separation step (blue; Fig. 2). The different MP (except the blue PE spheres) were placed in dry state on individual glass slides, imaged under the vis microscope and rinsed with 2 mL DI water into a 250 mL glass beaker. The sewage sludge samples (0.1 g or 1 g dry weight (dw)) were added to the glass beakers, and in the case of WH sludge, 50 mL of DI water were added. For the NG and synthetic sludge addition of DI water was not necessary as the water content of these samples was >95%. The filled glass beakers were incubated for 2 h on a horizontal shaker (100 rpm, Heidolph Incubator 1000/Unimax 1010) resulting in a well-mixed sewage sludge slurry.

The PP fibers and the PET fragments were larger than 100 μm and the recovery rates were determined by identification of the spiked polymers under the vis microscope (on the 100 μm stainless steel sieve). Recovery rates for PE spheres were assessed based on the extracts of spiked digested sewage sludge filtered on the Al_2O_3 membranes and investigated using (automated) vis microscopy and FPA-μ-FT-IR imaging (Fig. 2).

2.5.3. Method blanks

The following 3 matrices were processed the same way as the spiked samples and served as method blanks: i) unspiked WH and NG sludge (MB-WH and MB-NG, Table S2) to assess false positive detections of spiked (colored) PE spheres used as surrogate standards, ii) synthetic sludge samples (MB-syn, Table S2) to identify false positive detections of any type of MP and iii) DI water (MB-DI, Table S2) to evaluate the extent of MP contamination.

2.5.4. Measures to avoid contamination

Limiting contamination along the whole analytical chain is of key importance when quantifying MP contents from various matrices. In this work, however, the focus was on the recovery of clearly identifiable MP spiked to digested sewage sludge. For this reason, an excessive exclusion of laboratory utensils containing plastic materials was not required. Nevertheless, the following measures were taken to avoid MP contamination: Lab-coats made of cotton were worn at all times when samples were either processed or measured on the microscopes. The glass vials, petri dishes and the filtration funnels were always covered with aluminum foil. Plastic materials were avoided where possible (e.g., by using glass filtration devices), but pipettes and squirt bottles were still made of plastic.

2.6. Visible light microscopy

Although the μ-FT-IR system is equipped with a vis microscope, the lack of autofocusing routines, limited stitching capabilities and objectives with fixed magnifications made the use of a separate vis microscope mandatory. In this study, we used separate vis microscopes (SZX10, Olympus and VHX-7000, Keyence) to image MP in dry state (aliquots of powders deposited on glass slides), filtered from spiked DI water and filtered from extracts of spiked digested sewage sludge samples. PET fragments and PP fibers were always in the >100 μm fraction and counted under the vis microscope. The colored PE spheres (red and blue) were automatically detected on stitched images (recorded using the VHX-7000) of glass slides (PE spheres deposited in dry states) or Al_2O_3 membranes (filtered spiked DI water and filtered sludge extracts). The stitched images covered the entire filter area. In addition to the number, also the size of differently colored PE spheres was determined using image analysis tools.

2.7. Micro Fourier transform infrared spectroscopy (μ-FT-IR)

For the characterisation of MP before and after the digestion protocol, as well as for the identification of MP in the sludge extracts, a μ-FT-IR system (Cary 670 FTIR instrument, Cary 610 IR microscope, Agilent) was used. The system was equipped with an ATR unit for manual measurements and with a focal plane array detector (FPA, 64 × 64 detector elements) for automated measurements of larger areas. The 15× IR objective was used for all measurements. Measurements by ATR were performed from 4000 to 400 cm^{-1} at a spectral resolution of 4 cm^{-1}, the measurements and the background were both integrated 64 times. Analyses by FPA were conducted in transmission mode between 3900 and 1250 cm^{-1} at a spectral resolution of 8 cm^{-1}. The measurements were integrated 16 times and the background was integrated 64 times. The pixel resolution of the FPA measurements was 5.5 μm and thus one FPA measurement covered an area of 352 μm × 352 μm. For the Al_2O_3 membranes containing PE spheres from the spiked DI water, 4 areas each consisting of ~100 FPA measurements (3.5 mm × 3.5 mm) were recorded resulting in a total area of ~50 mm^2, or ~25% of the total filter area (192 mm^2). For the extracts of the spiked digested sewage sludge samples, 4 areas of ~200 FPA measurements (5 mm × 5 mm) were recorded resulting in a total area of ~100 mm^2 or ~50% of the total filter area. The recorded spectra from the FPA measurements were processed using the software Microplastics Finder (R2021a, Purency, Austria), which is based on a random decision forest algorithm (Hufnagl et al., 2019, 2022). Using this software, detected MP were separated into 21 different polymer types. In all experiments, the setting of the software to identify different polymers were identical (Relevance 0.3, Similarity 0.15).

The identified polymer types and the associated areas derived from the Microplastics Finder software code were exported as text files and further processed using Matlab (R2019b). To identify the spiked PE spheres on the FPA-μ-FT-IR images, the (high resolution) images from the VHX-7000, with automatically detected PE spheres, were projected on the FPA-μ-FT-IR images and the coordinates of the spiked PE spheres were determined. The MP sizes and polymer types at these coordinates were then obtained from the Microplastic Finder software.

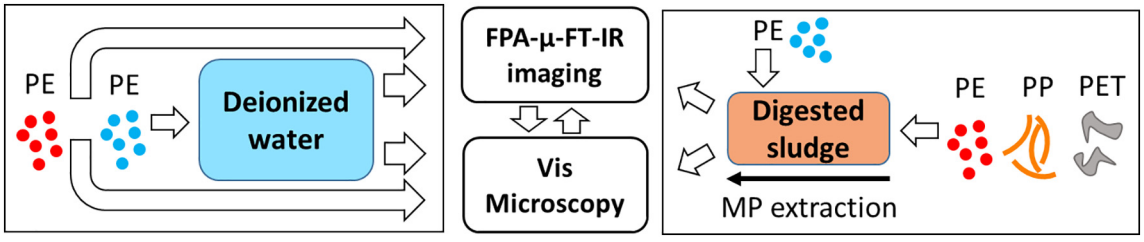

Fig. 2. Schematic of the approach to determine the recoveries over (parts of) the developed extraction method. Various particles were added over the extraction process: red and blue polyethylene (PE) spheres (~60 μm in diameter), orange polypropylene (PP) fibers (44 μm in diameter), and polyethylene terephthalate (PET) fragments (100 μm–200 μm in diameter). Red PE spheres also served as surrogate standards to determine number and size based recoveries in routine applications.

3. Results and discussion

3.1. Impact of the digestion protocol on the chemical structure and the morphology of the MP

Of key importance for the suitability of an extraction protocol for MP from solid matrices such as digested sewage sludge is an assessment of the changes of the chemical structure and the morphology caused by the different treatment steps. For that purpose, we recorded ATR FT-IR spectra and vis microscopy images of selected MP before and after oxidatively and enzymatically digesting the MP as described in the extraction protocol (Fig. 1).

The FT-IR spectra of all MP polymer types investigated in this study remained unaffected by the digestion procedures (Fig. 3). In agreement with the chemical structural preservation of the investigated polymer types during the digestion protocol, also the morphology and the coloration (red and blue PE spheres) of the MP mostly remained unaffected by the digestion procedures. Only polylactide (PLA) changed its appearance macroscopically; the surfaces became milky and the fibers more brittle (Fig. S1). Our results are, thus, in agreement with previous reports where enzymatic and/or oxidative treatments were used to digest organic materials without noticeable impacts on the polymer structures (Hurley et al., 2018; Li et al., 2018; Mintenig et al., 2017; Sujathan et al., 2017; Tagg et al., 2016).

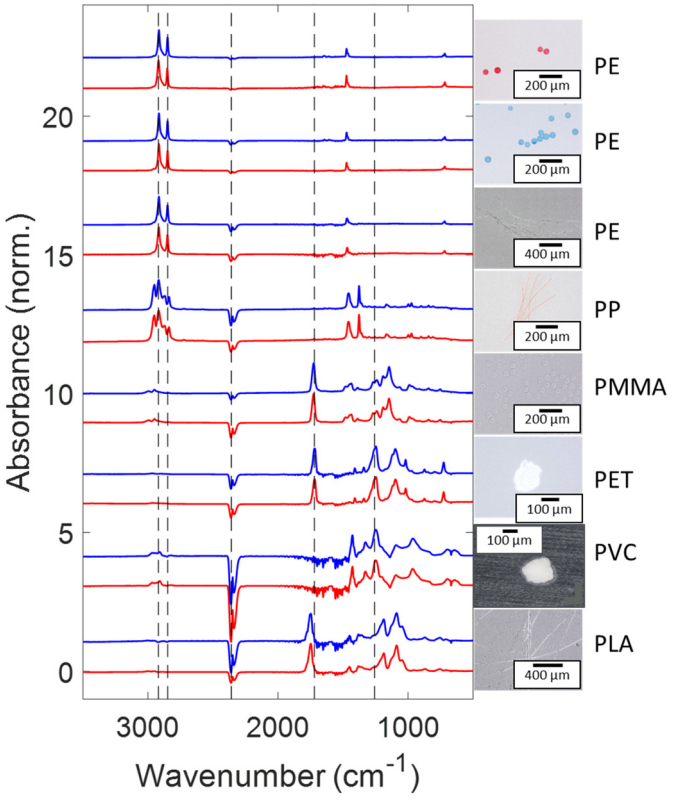

Fig. 3. ATR-FT-IR spectra of selected microplastic particles (MP) before and after oxidative and enzymatic digestion according to the optimized extraction protocol (for details, see text). Two spectra are provided for each MP type, the blue (upper) one representing the spectra recorded on the MP after the digestion procedure, the red (lower) one representing the spectrum of the pristine MP. The offset between the pristine and the 'aged' spectra is 1.1 normalized absorption units and the offset between the spectra of the different polymer types is 3. Vertical dashed lines at 2920, 2848, 2359, 1720 and 1257 cm^{-1} are guides to the eye. Visible light microscopy images of the pristine MP particles are provided to the right of the spectra and larger images are provided in Fig. S1. PET: polyethylene terephthalate, PP: polypropylene, PE: polyethylene, PMMA: polymethylmethacrylate, PVC: polyvinylchloride, PLA: polylactide.

3.2. Recovery of spiked MP

3.2.1. MP specific recovery based on visible light microscopy

The average recoveries of the fragments, spheres and fibers were between 80% and 100% over the whole analytical procedure for both experiments conducted using 0.1 g and 1 g of digested sewage sludge (dry weight) (Fig. 4). The recoveries of the red and the blue PE spheres were very similar, suggesting that MP can be kept in the extract during the digestion processes and were either lost during the density separation procedure or remained undetected during the following vis microscopy and FPA-μ-FT-IR analyses. The reason for a loss during the density separation procedure may be an aggregation between the PE particles and other particulate materials (heteroaggregation), followed by sedimentation.

In the method blanks conducted with DI water (MB-DI, Table S2) and synthetic sludge (MB-syn, Table S2), false positives did neither occur for blue nor for red PE spheres. In experiments where unspiked sewage sludge was extracted and analyzed (MB-NG and MB-WH, Table S2), 3 (1 g digested sewage sludge) and 1 (0.1 g digested sewage sludge) false positive PE spheres (red) used as surrogate standards were observed in total (3–4 replicates) resulting in roughly 1 false positive per replicate. In comparison to the total number of red PE spheres spiked to any given sample (33 on average) the false positives were a few percent only. The false positives are related to the automated sphere identification. In rare cases particles with a similar shape, color and size as the spiked PE spheres occurred in the sludge leading to an erroneous assignment of these particles. An example of such a particle is provided in Fig. S2.

3.2.2. Comparison of the visible light microscopy and the FPA-μ-FT-IR data

In the previous section, we demonstrated that spiked PE spheres remained in the extract and can be automatically detected by vis microscopy. However, the quantification of the MP content in complex matrices requires an identification of the chemical structure and an assessment of the size of the MP extracted from the respective matrices. The results from vis microscopy analyses (number, size, color) and from FPA-μ-FT-IR imaging (number, size, chemical structure) are summarized in Fig. 5 and discussed in the following sections.

3.2.2.1. Size and number of PE spheres in dry state. 116 (red) and 98 (blue) spheres were deposited in dry state on the glass slide. The size distribution of both MP types was very similar with a median diameter of 54 μm for the red and 56 μm for the blue spheres. The median sizes of the PE spheres agreed well to the data from the supplier, which were 53 μm – 63 μm.

3.2.2.2. Size and number of PE spheres recovered from spiked DI water (experiment 'DI water', Table S2). After transferring these PE spheres from the glass slides into DI water and filtering the suspensions on Al_2O_3 membranes, 100 (red) and 91 (blue) PE spheres were detected using automated vis microscopy, corresponding to a recovery of 86% for the red and 93% for the blue PE spheres. The median diameter of the red and the blue PE spheres were 58 μm and 67 μm, and thus significantly larger compared to the median diameter of the respective PE spheres determined on the glass slides (calculated based on a two-sample *t*-test at the 5% significance level). The PE spheres were deposited on either glass slides or on Al_2O_3 filter membranes and these two substrates provide a different (background) color. The spiked PE spheres (red and blue) are detected based on the contrast between the color of the particles and the color of the background. Slightly different degrees of contrasts between the glass slides and the PE spheres compared to the Al_2O_3 filter membranes and the PE spheres may result in different threshold levels for particle detection and eventually in slight differences in the area of the individual particles identified by the software. The similar recovery in terms of number and size, however, underlines that the two types of PE spheres can reliably be distinguished using automated vis microscopy.

Based on the FPA-μ-FT-IR imaging 41 PE spheres (red and blue) were detected or 151 when scaled to the total filter area, resulting in a recovery rate of 71%. This recovery rate is lower compared to the recovery rates

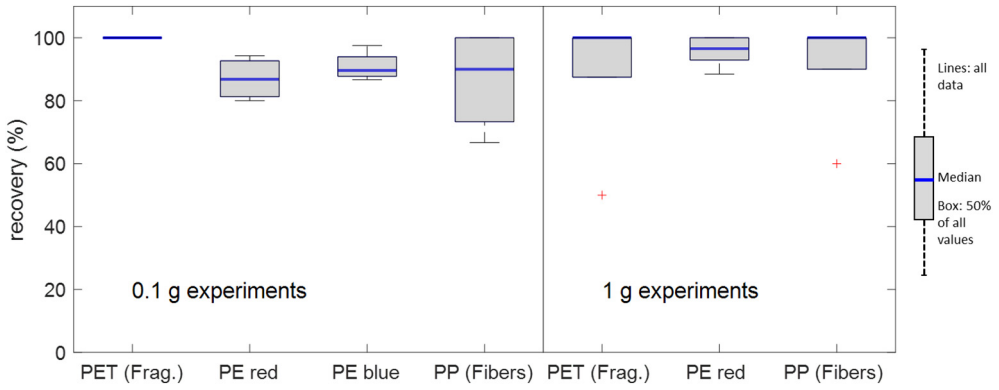

Fig. 4. Microplastic particle (MP) specific recovery rates for sewage sludge matrices (sludge WH and sludge NG samples, Table S2). MP in the extracts were detected under a visible light microscope either visually (fragments and fibers) or using automated image analysis tools (colored PE spheres). In total 22 PET fragments, 296 PE spheres (red), 199 PE spheres (blue) and 73 PP fibers were spiked to the sludge matrices. Occasionally, individual (1–3) red and blue PE spheres were detected on the 100 μm stainless steel grid. These PE spheres were also included in the calculation of the recoveries.

determined based on the vis microscopy data, which were around 90%. We assume that the lower recovery was related to an uneven deposition pattern of the PE spheres on the Al_2O_3 membranes, resulting in a lower recovery when scaling the number counts to the total filter area. The size of the PE spheres (red and blue) derived from the FPA-μ-FT-IR imaging of the Al_2O_3 membranes was with a median diameter of 54 μm in good agreement with the results from the vis microscopy.

3.2.2.3. Size and number of PE spheres recovered from spiked digested sewage sludge (experiment 'Sludge WH 2.2', Table S2). Out of 15 red PE spheres that were spiked to the digested sludge, 11 and 6 (12 when scaled to the total filter area) were detected on filtered sludge extracts by vis microscopy and FPA-μ-FT-IR imaging, respectively. Furthermore, out of 83 blue PE spheres that were spiked to the sludge extracts after the digestion steps but before the density separation, 73 and 35 (68 when scaled to the total filter area) were identified by vis microscopy and FPA-μ-FT-IR imaging, respectively. This translates into similar recovery rates of around 80% for the blue and for the red PE spheres by either vis microscopy and FPA-μ-FT-IR imaging (Fig. 5).

The median size of the PE spheres extracted from the spiked digested sewage sludge (red) and from the spiked sludge extracts after the digestion but before the density separation process (blue) determined by vis microscopy was 46 μm and 65 μm, respectively. Again, the median diameter of the blue PE spheres derived from the vis microscopy data were larger compared to the median diameter of the red PE spheres, consistent with the results obtained from the spiked DI water samples. The median diameter of the red and blue PE spheres derived from the FPA-μ-FT-IR imaging (note: the FPA-μ-FT-IR imaging only provides information about the size and the chemical structure of the MP. Detected PE spheres were thus separated into red and blue PE spheres according to the data from the vis microscopy analyses) was 59 μm and 61 μm respectively. These results are in good agreement with the results from the vis microscopy and with the results from the PE spheres spiked to and recovered from DI water, where PE spheres from the same stock powders were used (Fig. 5).

In conclusion, results from both automated vis microscopy and FPA-μ-FT-IR imaging showed that the number based recovery rate for spiked PE spheres over the whole analytical chain was around 80% and that the median size of the PE spheres recovered from extracts of the spiked sludge was similar to the median sizes of the PE spheres in the stock powders. This demonstrated the suitability of colored PE spheres as surrogate standards.

3.3. MP contents in digested sludge and comparison with other studies

After having i) assessed the stability of different MP types during the developed extraction protocol, ii) quantified the recoveries of MP based on spiking experiments in combination with automated vis microscopy and FPA-μ-FT-IR measurements, and iii) demonstrated that the size of MP can successfully be derived from FPA-μ-FT-IR imaging, we considered the established analytical protocol ready for routine application. Hence, one replicate experiment where PE spheres were spiked as surrogate standards to

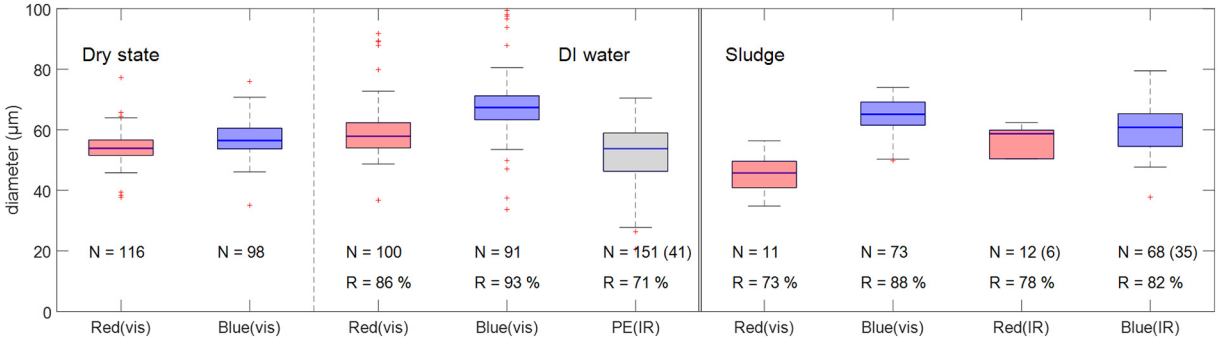

Fig. 5. Boxplots of the size of the polyethylene (PE) spheres that were deposited on glass slides ('Dry state'), spiked to deionized water and filtered on Al_2O_3 membranes ('DI water', same particles as for 'Dry state')) or extracted from spiked digested sewage sludge and filtered on Al_2O_3 membranes ('Sludge', referring to data from experiment 'Sludge WH 2.2', Table S2). The number of particles detected (N) and the calculated recovery rates (R) with respect to the number of spiked PE spheres detected on the glass slides are provided at the bottom of the figure. Numbers in brackets refer to the number counts, which were scaled to the total filter area (FPA-μ-FT-IR measurements). 'vis' and 'IR' refer to data derived from visible light microscopy analyses and from FPA-μ-FT-IR imaging, respectively. In the 'Sludge' experiment, 15 red PE spheres were spiked to the digested sludge and 83 blue PE spheres to the extracts after the enzymatic digestion.

sewage sludge was exemplarily analyzed for its MP contents using FPA-μ-FT-IR imaging.

PE, PP and PET were the most prominent polymer types in all but the smallest size bin (Figs. 6 and S3). In the smallest size bin, corresponding to the MP with a circular equivalent diameter between 20 μm and 30 μm, polyamides (PA) were most prominent. In the following size bin (30 μm–40 μm), PA MP were only of minor importance. The dominant polymer types (PE, PP, PA, PET) identified in the sludge samples reflect the high production volume of these materials (Plastics Europe, 2021) and is consistent with other reports of polymer types in sewage sludge samples (Enfrin et al., 2019 (and references therein)).

The total number of particles - in our study spanning a size range between 20 μm and 160 μm (circular equivalent diameter) - amounted to about 650 (exact: 664), which, when scaled to the total filter area (99 mm^2 area scanned, total area 192 mm^2) amounts to roughly 1300 particles in 0.1 g (dry basis) of digested sewage sludge. With about 10,000 #/g, the MP number concentration in sewage sludge observed in this study is higher compared to most other reports. MP number concentrations were around a few to a few tens or hundreds of MP per g in dried sewage sludge (Blaesing and Amelung, 2018; Leslie et al., 2017; Li et al., 2018; Mahon et al., 2017; Mintenig et al., 2017; Sujathan et al., 2017). Most recently, however, Horton et al. (2021) reported MP number concentrations of up to 10,000 #/g (dried sewage sludge), which is very similar to our results. This suggests that older studies, where MP were mainly detected on a manual basis, may have greatly underestimated the MP number concentrations in sewage sludge. Furthermore, Simon et al. (2018) reported MP number concentrations of up to 10,000 #/L in raw wastewater. Using typical total suspended solids (TSS) concentrations of a few 100 mg/L in untreated wastewater (Gujer, 2007), this translates into up to 100,000 #/g of dry weight. Reported concentrations of MP particles in treated wastewater range from 10^{-2} to 10^{4} #/L (Koelmans et al., 2019), which - assuming a total solid content of 5 mg/L in the treated wastewater - translates into a concentration of up to 10^{6} #/g, which is two orders of magnitudes above our results. The most plausible reasons for the apparent discrepancies between different studies in the reported MP concentrations are different size detection limits, different degrees of automation and most likely also different recoveries, which have unfortunately never been determined on a sample specific basis in previous studies. When assessing the sample specific recoveries, especially using automated systems, it is essential to evaluate the recoveries also based on these same systems, e.g., when using an FPA-μ-FT-IR system, the recovery for both size and number concentrations also has to be determined using the FPA-μ-FT-IR technology. Introducing a surrogate standard as a routine QA/QC measure (e.g., by adding colored PE spheres), will allow the comparison and interpretation of data from different studies using different analytical methods.

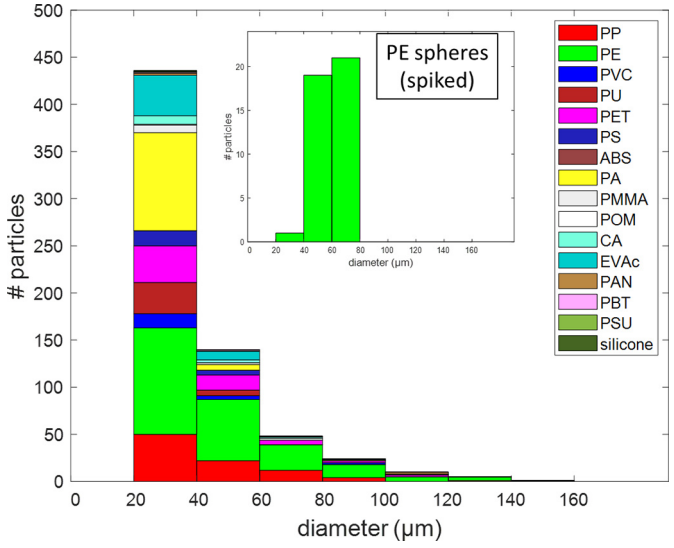

Fig. 6. Polymer specific particle size distribution (PSD) of the identified, native microplastic particles (MP) extracted from 0.1 g (dry weight basis) of digested sewage sludge (Experiment 'Sludge WH 2.2', Table S2). The PSD of individual polymers is provided in the SI (Fig. S3). The inset shows the spiked polyethylene (PE) spheres that were detected in the extracts. These PE spheres were excluded from the PSD. For abbreviations of individual MP polymer types, see Text and Table S3.

Method blanks (DI water and synthetic (MP 'free') sludge) digested the same way as the experimental samples both resulted in low total MP number concentrations of around 10 particles per 5 × 5 mm^2, corresponding to about 80 particles per filter (192 mm^2, Figs. S4 and S5). Hence, the MP introduced by either contamination or false positives contribute to about 5% to the total number of MP detected in the digested sewage sludge samples. In both method blanks - DI water (MB-DI) and synthetic sludge (MB-syn) - polyamid (PA) particles were detected. Apart from PA, different types of polymers were found in these two blank samples. However, the interpretation of low MP number counts as observed in this study is challenging and the polymer types and numbers in blank samples will have to be monitored over an extended period of time for a reliable interpretation of these data.

4. Conclusions

The chemical structure of the investigated MP, covering the most commonly used polymer types, remained unaffected by the developed extraction protocol and morphological changes were only observed for PLA fibers. The developed sample preparation approach successfully removed easily digestible material and efficiently separated inorganic particles of higher density from the sludge digests. Surrogate standards in the form of colored PE spheres spiked to digested sludge samples during routine application, allowed the determination of sample specific recovery rates, both in terms of MP number and MP size and, as such, constitute a QA/QC quality control instrument for routine MP quantification.

There is a consensus amongst scientists that harmonized and validated sample preparation protocols have to be developed to better assess MP pollution in different environmental compartments. Based on the data of this study, we argue that an assessment of sample specific recoveries is as important as validated sample preparation procedures. Often, researchers are challenged by demanding sample matrices requiring the adoption of published sample preparation schemes. It is, therefore, of key importance to have QA/QC on the individual sample level, which makes the addition of a surrogate standard mandatory. The approach described in this paper goes along these arguments and can be extended to also include particles of smaller and larger diameters. In the future, we envision using a multitude of PE spheres of different sizes and colors to constrain the sample specific MP recoveries on a largely automated basis. The assessment of the samples specific recoveries using automated vis microscopy requires roughly 15 min, which is negligible compared to the FPA-μ-FT-IR analysis lasting several hours. The initial screening of the samples and the determination of the specific MP recoveries, thus, will also save time as ill prepared samples can quickly be identified and do not need to be further analyzed using more time consuming analytical techniques. Our novel approach of spike-recovery experiments using colored PE spheres can be adapted to other matrices (e.g., soils, sediments, food) and may, thus, become a cornerstone for QA/QC measures for MP analysis under routine conditions.

CRediT authorship contribution statement

Matthias Philipp: Project administration, Investigation, Data curation, Writing - original draft, **Thomas D. Bucheli:** Conceptualization, Writing - review & editing, **Ralf Kaegi:** Funding acquisition, Conceptualization, Project administration, Writing - review & editing.

Declaration of competing interest

The authors declare that they have no known competing financial interests or personal relationships that could have appeared to influence the work reported in this paper.

Acknowledgements

The authors would like to thank Brian Sinnet for support in the laboratory. We are indebted to the Swiss Federal Office for the Environment for financial support (Grant No. 19.0011.PJ/13E464FD9).

Appendix A. Supplementary data

Supplementary data to this article can be found online at https://doi.org/10.1016/j.scitotenv.2022.155485.

References

Ali, I., Ding, T., Peng, C., Naz, I., Sun, H., Li, J., Liu, J., 2021. Micro- and nanoplastics in wastewater treatment plants: occurrence, removal, fate, impacts and remediation technologies – a critical review. Chem. Eng. J. 423, 130205. https://doi.org/10.1016/j.cej.2021.130205.

Andrady, A.L., 2011. Microplastics in the marine environment. Mar. Pollut. Bull. 62, 1596–1605. https://doi.org/10.1016/j.marpolbul.2011.05.030.

Andrady, A.L., 2017. The plastic in microplastics: a review. Mar. Pollut. Bull. 119, 12–22. https://doi.org/10.1016/j.marpolbul.2017.01.082.

Anger, P.M., von der Esch, E., Baumann, T., Elsner, M., Niessner, R., Ivleva, N.P., 2018. Raman microspectroscopy as a tool for microplastic particle analysis. TrAC Trends Anal. Chem. 109, 214–226. https://doi.org/10.1016/j.trac.2018.10.010.

Barnes, D.K.A., Galgani, F., Thompson, R.C., Barlaz, M.A., 2009. Accumulation and fragmentation of plastic debris in global environments. Philos. Trans. R. Soc. B https://doi.org/10.1098/rstb.2008.0205.

Beaurepaire, M., Dris, R., Gasperi, J., Tassin, B., 2021. Microplastics in the atmospheric compartment: a comprehensive review on methods, results on their occurrence and determining factors. Curr. Opin. Food Sci. 41, 159–168. https://doi.org/10.1016/j.cofs.2021.04.010.

Ben-David, E.A., Habibi, M., Haddad, E., Hasanin, M., Angel, D.L., Booth, A.M., Sabbah, I., 2021. Microplastic distributions in a domestic wastewater treatment plant: removal efficiency, seasonal variation and influence of sampling technique. Sci. Total Environ. 752, 141880. https://doi.org/10.1016/j.scitotenv.2020.141880.

Birch, Q.T., Potter, P.M., Pinto, P.X., Dionysiou, D.D., Al-Abed, S.R., 2020. Sources, transport, measurement and impact of nano and microplastics in urban watersheds. Rev. Environ. Sci. Biotechnol. 19, 275–336. https://doi.org/10.1007/s11157-020-09529-x.

Blaesing, M., Amelung, W., 2018. Plastics in soil: analytical methods and possible sources. Sci. Total Environ. 612, 422–435. https://doi.org/10.1016/j.scitotenv.2017.08.086.

Browne, M.A., Galloway, T., Thompson, R., 2007. Microplastic—an emerging contaminant of potential concern? Integr. Environ. Assess. Manag. 3, 559–561. https://doi.org/10.1002/ieam.5630030412.

Campanale, C., Galafassi, S., Savino, I., Massarelli, C., Ancona, V., Volta, P., Uricchio, V.F., 2022. Microplastics pollution in the terrestrial environments: poorly known diffuse sources and implications for plants. Sci. Total Environ. 805, 150431. https://doi.org/10.1016/j.scitotenv.2021.150431.

Carr, S.A., Liu, J., Tesoro, A.G., 2016. Transport and fate of microplastic particles in wastewater treatment plants. Water Res. 91, 174–182. https://doi.org/10.1016/j.watres.2016.01.002.

Cole, M., Webb, H., Lindeque, P.K., Fileman, E.S., Halsband, C., Galloway, T.S., 2014. Isolation of microplastics in biota-rich seawater samples and marine organisms. Sci. Rep. 4, 4528. https://doi.org/10.1038/srep04528.

Conley, K., Clum, A., Deepe, J., Lane, H., Beckingham, B., 2019. Wastewater treatment plants as a source of microplastics to an urban estuary: removal efficiencies and loading per capita over one year. Water Res. X 3, 100030. https://doi.org/10.1016/j.wroa.2019.100030.

Duis, K., Coors, A., 2016. Microplastics in the aquatic and terrestrial environment: sources (with a specific focus on personal care products), fate and effects. Environ. Sci. Eur. 28, 1–25. https://doi.org/10.1186/s12302-015-0069-y.

Enfrin, M., Dumee, L.F., Lee, J., 2019. Nano/microplastics in water and wastewater treatment processes - origin, impact and potential solutions. Water Res. 161, 621–638. https://doi.org/10.1016/j.watres.2019.06.049.

Fonts, I., Azuara, M., Gea, G., Murillo, M.B., 2009. Study of the pyrolysis liquids obtained from different sewage sludge. J. Anal. Appl. Pyrolysis 85, 184–191. https://doi.org/10.1016/j.jaap.2008.11.003.

Gatidou, G., Arvaniti, O.S., Stasinakis, A.S., 2019. Review on the occurrence and fate of microplastics in sewage treatment plants. J. Hazard. Mater. 367, 504–512. https://doi.org/10.1016/j.jhazmat.2018.12.081.

Geyer, R., Jambeck, J.R., Law, K.L., 2017. Production, use, and fate of all plastics ever made. Sci. Adv. 3, e1700782. https://doi.org/10.1126/sciadv.1700782.

Gujer, W., 2007. Siedlungswasserwirtschaft. 3rd ed. Springer-Verlag, Berlin Heidelberg https://doi.org/10.1007/978-3-540-34330-1.

Han, X., Lu, X., Vogt, R.D., 2019. An optimized density-based approach for extracting microplastics from soil and sediment samples. Environ. Pollut. 254, 113009. https://doi.org/10.1016/j.envpol.2019.113009.

Hartmann, N.B., Hüffer, T., Thompson, R.C., Hassellöv, M., Verschoor, A., Daugaard, A.E., Rist, S., Karlsson, T., Brennholt, N., Cole, M., Herrling, M.P., Hess, M.C., Ivleva, N.P., Lusher, A.L., Wagner, M., 2019. Are we speaking the same Language? Recommendations for a definition and categorization framework for plastic debris. Environ. Sci. Technol. 53, 1039–1047. https://doi.org/10.1021/acs.est.8b05297.

He, D., Luo, Y., Lu, S., Liu, M., Song, Y., Lei, L., 2018. Microplastics in soils: analytical methods, pollution characteristics and ecological risks. TrAC Trends Anal. Chem. 109, 163–172. https://doi.org/10.1016/j.trac.2018.10.006.

Hidalgo, M., Uheida, A., Salvadó, V., Fontàs, C., 2006. Study of the sorption and separation abilities of commercial solid-phase extraction (SPE) cartridge oasis MAX towards Au (III), Pd(II), Pt(IV), and Rh(III). Solvent Extr. Ion Exch. 24, 931–942. https://doi.org/10.1080/07366290600952733.

Horton, A.A., Walton, A., Spurgeon, D.J., Lahive, E., Svendsen, C., 2017. Microplastics in freshwater and terrestrial environments: evaluating the current understanding to identify the knowledge gaps and future research priorities. Sci. Total Environ. 586, 127–141. https://doi.org/10.1016/j.scitotenv.2017.01.190.

Horton, A.A., Cross, R.K., Read, D.S., Jürgens, M.D., Ball, H.L., Svendsen, C., Vollertsen, J., Johnson, A.C., 2021. Semi-automated analysis of microplastics in complex wastewater samples. Environ. Pollut. 268, 115841. https://doi.org/10.1016/j.envpol.2020.115841.

Hufnagl, B., Steiner, D., Renner, E., Löder, M.G.J., Laforsch, C., Lohninger, H., 2019. A methodology for the fast identification and monitoring of microplastics in environmental samples using random decision forest classifiers. Anal. Methods 11, 2277–2285. https://doi.org/10.1039/C9AY00252A.

Hufnagl, B., Stibi, M., Martirosyan, H., Wilczek, U., Möller, J.N., Löder, M.G.J., Laforsch, C., Lohninger, H., 2022. Computer-assisted analysis of microplastics in environmental samples based on μFTIR imaging in combination with machine learning. Environ. Sci. Technol. Lett. 9, 90–95. https://doi.org/10.1021/acs.estlett.1c00851.

Hurley, R.R., Lusher, A.L., Olsen, M., Nizzetto, L., 2018. Validation of a method for extracting microplastics from complex, organic-rich, environmental matrices. Environ. Sci. Technol. 52, 7409–7417. https://doi.org/10.1021/acs.est.8b01517.

Ivleva, N.P., Wiesheu, A.C., Niessner, R., 2017. Microplastic in aquatic ecosystems. Angew. Chem.-Int. Ed. 56, 1720–1739. https://doi.org/10.1002/anie.201606957.

Jambeck, J.R., Geyer, R., Wilcox, C., Siegler, T.R., Perryman, M., Andrady, A., Narayan, R., Law, K.L., 2015. Plastic waste inputs from land into the ocean. Science 347, 768–771. https://doi.org/10.1126/science.1260352.

Junhao, C., Xining, Z., Xiaodong, G., Li, Z., Qi, H., Siddique, K.H.M., 2021. Extraction and identification methods of microplastics and nanoplastics in agricultural soil: a review. J. Environ. Manag. 294, 112997. https://doi.org/10.1016/j.jenvman.2021.112997.

Kirstein, I.V., Hensel, F., Gomiero, A., Iordachescu, L., Vianello, A., Wittgren, H.B., Vollertsen, J., 2021. Drinking plastics? – quantification and qualification of microplastics in drinking water distribution systems by μFTIR and py-GCMS. Water Res. 188, 116519. https://doi.org/10.1016/j.watres.2020.116519.

Kloeckner, P., Reemtsma, T., Eisentraut, P., Braun, U., Ruhl, A.S., Wagner, S., 2019. Tire and road wear particles in road environment - quantification and assessment of particle dynamics by zn determination after density separation. Chemosphere 222, 714–721. https://doi.org/10.1016/j.chemosphere.2019.01.176.

Koelmans, A.A., Mohamed Nor, N.H., Hermsen, E., Kooi, M., Mintenig, S.M., De France, J., 2019. Microplastics in freshwaters and drinking water: critical review and assessment of data quality. Water Res. 155, 410–422. https://doi.org/10.1016/j.watres.2019.02.054.

Kumar, M., Xiong, X., He, M., Tsang, D.C.W., Gupta, J., Khan, E., Harrad, S., Hou, D., Ok, Y.S., Bolan, N.S., 2020. Microplastics as pollutants in agricultural soils. Environ. Pollut. 265, 114980. https://doi.org/10.1016/j.envpol.2020.114980.

Leslie, H.A., Brandsma, S.H., van Velzen, M.J.M., Vethaak, A.D., 2017. Microplastics en route: field measurements in the dutch river delta and Amsterdam canals, wastewater treatment plants, North Sea sediments and biota. Environ. Int. 101, 133–142. https://doi.org/10.1016/j.envint.2017.01.018.

Li, X., Chen, L., Mei, Q., Dong, B., Dai, X., Ding, G., Zeng, E.Y., 2018. Microplastics in sewage sludge from the wastewater treatment plants in China. Water Res. 142, 75–85. https://doi.org/10.1016/j.watres.2018.05.034.

Löder, M.G.J., Kuczera, M., Mintenig, S., Lorenz, C., Gerdts, G., 2015. Focal plane array detector-based micro-fourier-transform infrared imaging for the analysis of microplastics in environmental samples. Environ. Chem. 12, 563–581. https://doi.org/10.1071/EN14205.

Mahon, A.M., O'Connell, B., Healy, M.G., O'Connor, I., Officer, R., Nash, R., Morrison, L., 2017. Microplastics in sewage sludge: effects of treatment. Environ. Sci. Technol. 51, 810–818. https://doi.org/10.1021/acs.est.6b04048.

Mintenig, S.M., Int-Veen, I., Löder, M.G.J., Primpke, S., Gerdts, G., 2017. Identification of microplastic in effluents of waste water treatment plants using focal plane array-based micro-fourier-transform infrared imaging. Water Res. 108, 365–372. https://doi.org/10.1016/j.watres.2016.11.015.

Mintenig, S.M., Löder, M.G.J., Primpke, S., Gerdts, G., 2019. Low numbers of microplastics detected in drinking water from ground water sources. Sci. Total Environ. 648, 631–635. https://doi.org/10.1016/j.scitotenv.2018.08.178.

Moeller, J.N., Löder, M.G.J., Laforsch, C., 2020. Finding microplastics in soils – a review of analytical methods. Environ. Sci. Technol. https://doi.org/10.1021/acs.est.9b04618.

Möller, J.N., Heisel, I., Satzger, A., Vizsolyi, E.C., Oster, S.D.J., Agarwal, S., Laforsch, C., Löder, M.G.J., 2021. Tackling the challenge of extracting microplastics from soils: a protocol to purify soil samples for spectroscopic analysis. Environ. Toxicol. Chem. https://doi.org/10.1002/etc.5024 n/a.

Pico, Y., Alfarhan, A., Barcelo, D., 2019. Nano- and microplastic analysis: focus on their occurrence in freshwater ecosystems and remediation technologies. TrAC Trends Anal. Chem. 113, 409–425. https://doi.org/10.1016/j.trac.2018.08.022.

Plastics Europe, 2021. Plastics the facts. https://plasticseurope.org/wp-content/uploads/2021/12/Plastics-the-Facts-2021-web-final.pdf.

Primpke, S., Lorenz, C., Rascher-Friesenhausen, R., Gerdts, G., 2017. An automated approach for microplastics analysis using focal plane array (FPA) FTIR microscopy and image analysis. Anal. Methods 9, 1499–1511. https://doi.org/10.1039/C6AY02476A.

Primpke, S., Wirth, M., Lorenz, C., Gerdts, G., 2018. Reference database design for the automated analysis of microplastic samples based on fourier transform infrared (FTIR) spectroscopy. Anal. Bioanal. Chem. 410, 5131–5141. https://doi.org/10.1007/s00216-018-1156-x.

Primpke, S., Christiansen, S.H., Cowger, W., De Frond, H., Deshpande, A., Fischer, M., Holland, E.B., Meyns, M., O'Donnell, B.A., Ossmann, B.E., Pittroff, M., Sarau, G., Scholz-Böttcher, B.M., Wiggin, K.J., 2020. Critical assessment of analytical methods for the harmonized and cost-efficient analysis of microplastics. Appl. Spectrosc. 74, 1012–1047. https://doi.org/10.1177/0003702820921465.

Rasmussen, L.A., Iordachescu, L., Tumlin, S., Vollertsen, J., 2021. A complete mass balance for plastics in a wastewater treatment plant - macroplastics contributes more than microplastics. Water Res. 201, 117307. https://doi.org/10.1016/j.watres.2021.117307.

Schwabl, P., Köppel, S., Königshofer, P., Bucsics, T., Trauner, M., Reiberger, T., Liebmann, B., 2019. Detection of various microplastics in human stool. Ann. Intern. Med. 171, 453–457. https://doi.org/10.7326/M19-0618.

Simon, M., van Alst, N., Vollertsen, J., 2018. Quantification of microplastic mass and removal rates at wastewater treatment plants applying focal plane Array (FPA)-based fourier transform infrared (FT-IR) imaging. Water Res. 142, 1–9. https://doi.org/10.1016/j.watres.2018.05.019.

Stock, F., Kochleus, C., Bänsch-Baltruschat, B., Brennholt, N., Reifferscheid, G., 2019. Sampling techniques and preparation methods for microplastic analyses in the aquatic environment – a review. TrAC Trends Anal. Chem. 113, 84–92. https://doi.org/10.1016/j.trac.2019.01.014.

Sujathan, S., Kniggendorf, A.-K., Kumar, A., Roth, B., Rosenwinkel, K.-H., Nogueira, R., 2017. Heat and bleach: a cost-efficient method for extracting microplastics from return activated sludge. Arch. Environ. Contam. Toxicol. 73, 641–648. https://doi.org/10.1007/s00244-017-0415-8.

Sun, J., Dai, X., Wang, Q., van Loosdrecht, M.C.M., Ni, B.-J., 2019. Microplastics in wastewater treatment plants: detection, occurrence and removal. Water Res. 152, 21–37. https://doi.org/10.1016/j.watres.2018.12.050.

Tagg, A.S., Harrison, J.P., Ju-Nam, Y., Sapp, M., Bradley, E.L., Sinclair, C.J., Ojeda, J.J., 2016. Fenton's reagent for the rapid and efficient isolation of microplastics from wastewater. Chem. Commun. 53, 372–375. https://doi.org/10.1039/C6CC08798A.

Talvitie, J., Mikola, A., Koistinen, A., Setälä, O., 2017. Solutions to microplastic pollution – removal of microplastics from wastewater effluent with advanced wastewater treatment technologies. Water Res. 123, 401–407. https://doi.org/10.1016/j.watres.2017.07.005.

Thompson, R.C., Olsen, Y., Mitchell, R.P., Davis, A., Rowland, S.J., John, A.W.G., McGonigle, D., Russell, A.E., 2004. Lost at sea: where is all the plastic? Science 304. https://doi.org/10.1126/science.1094559 838-838.

Thompson, R., Moore, C., Andrady, A., Gregory, M., Takada, H., Weisberg, S., 2005. New directions in plastic debris. Science 310. https://doi.org/10.1126/science.310.5751.1117b 1117–1117.

Van Cauwenberghe, L., Devriese, L., Galgani, F., Robbens, J., Janssen, C.R., 2015. Microplastics in sediments: a review of techniques, occurrence and effects. Mar. Environ. Res. 111, 5–17. https://doi.org/10.1016/j.marenvres.2015.06.007.

Wielinski, J., Müller, C., Voegelin, A., Morgenroth, E., Kaegi, R., 2018. Combustion of sewage sludge: kinetics and speciation of the combustible. Energy Fuel 32, 10656–10667. https://doi.org/10.1021/acs.energyfuels.8b02106.

Zhou, Y., Wang, J., Zou, M., Jia, Z., Zhou, S., Li, Y., 2020. Microplastics in soils: a review of methods, occurrence, fate, transport, ecological and environmental risks. Sci. Total Environ. 748, 141368. https://doi.org/10.1016/j.scitotenv.2020.141368.